ChemComm

In Situ Synthesis of Fe3S4/MIL-53(Fe) hybrid catalyst for Efficient Electrocatalytic Hydrogen Evolution

Journal:	*ChemComm*
Manuscript ID	CC-COM-02-2019-001433.R1
Article Type:	Communication

Journal Name

COMMUNICATION

In Situ Synthesis of Fe_3S_4/MIL-53(Fe) hybrid catalyst for Efficient Electrocatalytic Hydrogen Evolution

Received 00th January 20xx,
Accepted 00th January 20xx

DOI: 10.1039/x0xx00000x

www.rsc.org/

Dan-Dan Huang, Shuang Li,* Ya-Pan Wu, Jun-Hua Wei, Jing-Wei Yi, Hai-Meng Ma, Qi-Chun Zhang , Yun-Ling Liu and Dong-Sheng Li*

The development of efficient MOF-based electrocatalysts with good stability to produce hdyrogen is a great challenge in the field of sustainable energy conversion. Herein, we introduced a controlled in-situ sulfurization strategy to generate a highly active and stable hybrid catalyst containing good conductive Fe_3S_4 ultrasmall nanosheets attached on the surface of 3D MIL-53(Fe) for hydrogen evolution reaction in acidic solutions.

Hydrogen (H_2), as a renewable and high energy carrier, has been regarded as a promising candidate to solve the energy crisis and environmental problems caused by the severe consumption of traditional fossil fuels.[1] Among the existing strategies for hydrogen production, the electrocatalytic hydrogen evolution reaction ($2H^+ + 2e^- \rightarrow H_2$, HER) is considered as one of the most efficient pathways.[2] However, owing to Pt-based noble metal catalysts are too costly for large-scale HER applications.[3] It is thus imperative to develop new electrocatalysts with both cost-effective and excellent HER activity.

In recent years, thanks to high surface areas, unique ordered porous structure, rich and readily accessible active sites, metal–organic frameworks (MOFs) have been regarded as good HER catalyst candidates.[4] However, most kinds of pristine MOFs suffer from the low conductivity and weak stability in the acidic/alkaline electrolyte,[5] which largely limit their applications in the HER. Although MOFs in their pristine form have rarely been applied as electrocatalysts, transition metal sulfides with high conductivity and reactivity derived from MOFs-based precursors have attracted intense research interest in HER application.[6] Nevertheless, the large surface area and well-defined pore/channel structures of MOF precursors are usually destroyed during the formation of their derivatives, which usually lead to the decrease of active sites.[7] Therefore, balancing the benefits between good conductivity and rich active sites is the most promising but challenging task for developing efficient MOF-based HER electrocatalysts.

To overcome this obstacle, we consider that it would be an effective method to realize the simultaneous modulations of both conductivity and active sites by incorporating MOF derivative - metal sulfide within MOF crystal material, which could combine the merits and cover the shortcomings of individual component. Moreover, the interaction between them could further improve HER activity. With these facts in mind, the partial sulfurization treatment using MOF material as a precursor could be an ideal strategy[8] to obtain the above MOF-based composites, which are expected to construct strong interaction between MOF and metal sulfide. Recently reported MIL-53(Fe) with one-dimensional (1D) channels and a flexible structure provided inspiration as a potential HER substrate for mass diffusion.[9] Furthermore, the MIL-53(Fe) constructed by high metal ions valence (FeO_6) and cheap organic ligands (1, 4-bezenedicarboxylate, 1, 4-BDC), possesses much stable structural frameworks and can be easily fabricated features[10] that make it an ideal precursor to synthesize MOF-based composite catalysts. Through controlled partial sulfurization treatment, iron-based sulfide with high conductivity[11] could be gradually generated from MIL-53(Fe) template, which is valuable for increasing the conductivity and the HER performance. Inspired by the above insight, the incorporation of iron-based sulfide with MIL-53(Fe) would be an effective solution to improve the catalytic activity of HER.

Herein, we reported a facile in-situ sulfurization strategy to synthesize highly active and stable MOF-metal sulfide composites for HER. By a simple solvothermal method, various amounts of ultrasmall Fe_3S_4 nanosheets attached on the surface of three-dimensional (3D) MIL-53(Fe) framework (named Fe_3S_4(*x* wt%)/MIL-53) hybrid catalysts were prepared. These hybrid catalysts retained the skeleton structure of the MOF while creating high conductivity and stable metal sulfide, which could take advantage of the merits of both components and the interaction between them, leading to the improved HER activity. By modulating the degrees of sulfurization, the

College of Materials and Chemical Engineering, Key Laboratory of Inorganic Nonmetallic Crystalline and Energy Conversion Materials, China Three Gorges University, Yichang, 443002, P. R. China. E-mail: lishmail@126.com; lidongshengl@126.com

† Electronic Supplementary Information (ESI) available: See DOI: 10.1039/x0xx00000x

optimized Fe_3S_4(52.1wt%)/MIL-53 hybrid catalyst with ideal hierarchical nanostructure and composition was identified, which possesses both rich effective active sites and high overall conductivity. As expected, the Fe_3S_4(52.1wt%)/MIL-53 hybrid catalyst exhibits a low overpotential of 92 mV at a current density of 10 mA cm^{-2}, a small Tafel slope of 60 mV $decade^{-1}$ and long term stability in acid solutions. This work provides a new method for designing efficient and stable MOF-based electrocatalysts for HER.

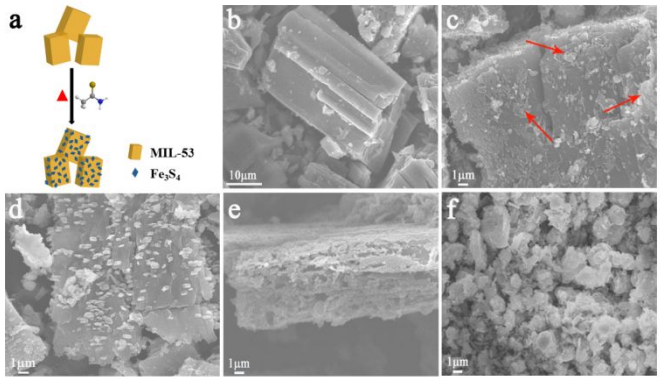

Fig. 1 (a) Schematic illustration of synthesis of Fe_3S_4(*x* wt%)/MIL-53 hybrid catalyst. (b-f) SEM images of Fe_3S_4(*x* wt%)/MIL-53 (*x* = 0, 31.3, 43.2, 52.1, 82.8) hybrid catalyst, respectively.

In this work, the synthetic procedure of Fe_3S_4(*x* wt%)/MIL-53 hybrid catalyst is illustrated in Fig. 1a. Briefly, the bulk MIL-53(Fe) precursors were first synthesized by a previously reported method with a few modifications (see the Experimental Section for details in the Supporting Information). Then, after one-pot well-controlled solvothermal reaction between the obtained bulk MIL-53(Fe) with thioacetamide (TAA) in EtOH solution, the hybrid catalyst composed of ultra-small Fe_3S_4 nanosheets attached on the surface of 3D bulk MIL-53(Fe) was prepared. In addition, as the reaction time and temperature increase, the amount and size of Fe_3S_4 nanosheets gradually increase with the dissolution of the inner MIL-53(Fe) template. Here, with a fixed concentration of substrates for sulfidation treatment 3 h at 140 °C, 160 °C, 180 °C, and 5 h at 180 °C, the four samples of Fe_3S_4(*x* wt%)/MIL-53 (*x* = 31.3, 43.2, 52.1, 82.8) hybrid catalyst were obtained, whose concentrations are determined by inductively coupled plasma mass spectrometry.

The morphological evolution of the samples at different periods of sulfidation treatment was characterized by Field emission scanning electron microscope (FE-SEM). As shown in Fig. 1b, the obtained MIL-53(Fe) precursor has 3D bulk structure with solid nature and smooth surface. After reacting with TAA for 3 h at 140 °C, the surface of the MIL-53(Fe) becomes rough and ultra-small Fe_3S_4 nanosheets start to emerge from the MOF substrate (indicated by red arrows in Fig. 1c). The number of the nanosheets within MOF increases and voids appear obvious inside the 3D bulk after reaction at 160 °C (Fig. 1d). When the reaction temperature increases to 180 °C, the inner MIL-53(Fe) becomes vulnerable and its surface is completely covered by randomly oriented Fe_3S_4 nanosheets with the content of 52.1wt%, resulting in the formation of an ideal hierarchical nanostructure(Fig. 1e). However, when the reaction time is prolonged to 5 h at 180 °C, the skeleton structure of 3D MOF is almost destroyed with 82.8wt% of Fe_3S_4 nanosheets generated (Fig. 1f).

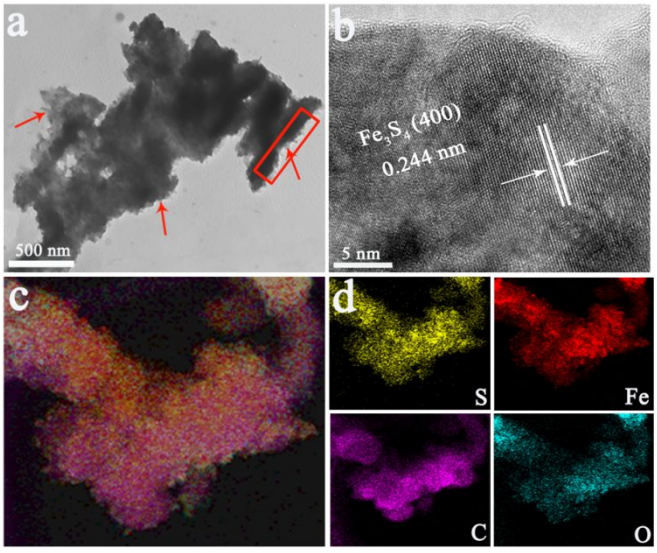

Fig. 2 TEM image (a), HRTEM image (b) and elemental mapping images (c-d) of the as-obtained Fe_3S_4(52.1wt%)/MIL-53 hybrid catalyst.

The hierarchical nanostructure of Fe_3S_4(52.1wt%)/MIL-53 hybrid catalyst was further confirmed by the transmission electron microscopy (TEM). As displayed in Fig. 2a, the ultra-small Fe_3S_4 nanosheets can be seen from the edge (indicated by red arrows). A corresponding high-resolution TEM (HRTEM) observation on the edge of the nanosheet (Fig 2b) clearly shows the well-crystalline nature with an interplanar distance of 0.244 nm, which corresponds to the (400) planes of the cubic Fe_3S_4 crystal structure, giving a direct evidence for the existence of Fe_3S_4 nanosheet in the hybrid catalyst. Moreover, elemental mapping analysis (Fig. 2c-d) of the obtained hybrid catalyst reveals the homogeneous distribution of C and O from MIL-53(Fe), S from Fe_3S_4, and Fe from both components.

X-ray diffraction (XRD) pattern and X-ray photoelectron spectra (XPS) were performed to confirm the phase composition, elemental compositions and the valence states of the Fe_3S_4(52.1wt%)/MIL-53 hybrid catalyst. As shown in Fig. 3a, all the diffraction peaks could be accordingly indexed to the cubic phase Fe_3S_4 (JCPDS Card No.16-0713) and MIL-53(Fe), confirming the coexisting phase of MIL-53(Fe) and Fe_3S_4 after sulfurization process without any residues and contaminants. Fig. 3b shows the XPS survey spectrum of the product, indicating the existence of elements Fe, S, C and O. For Fe 2p spectrum, the binding energies of 712.9 and 726.2 eV are attributed to Fe^{3+}, where the peaks at binding energies

of 711.2 and 724.5 eV are typical for Fe^{2+}.[12] Other peak at 720.1

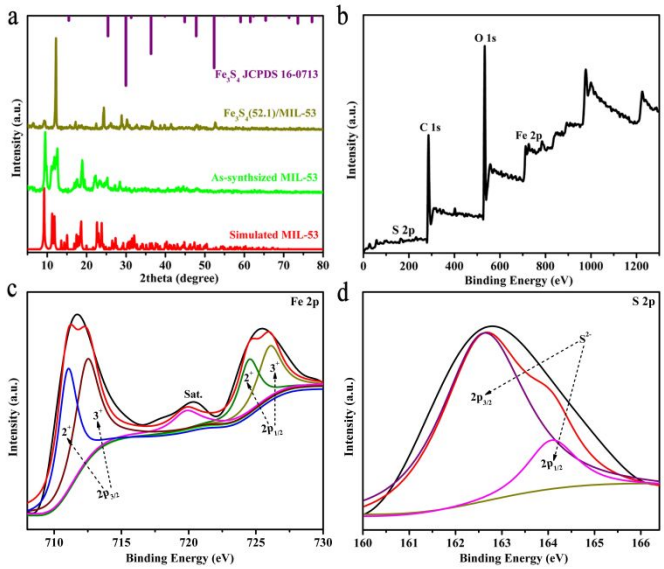

Fig. 3 (a) XRD pattern of the as-obtained Fe_3S_4(52.1wt%)/MIL-53 hybrid catalyst. XPS spectra of survey (b), Fe 2p (c), and S 2p (d) of the Fe_3S_4(52.1wt%)/MIL-53 hybrid catalyst.

eV can be assigned to the satellite peak for the above peaks. The XPS spectrum of S 2p could be fitted by two peaks at binding energies of around 162.6 and 164.1eV(Fig. 3d), which are assigned to the S^{2-} ions in Fe_3S_4 nanosheets.[11b] In addition, the Fourier transform infrared (FT-IR) spectra of the product in Fig. S2 clearly demonstrates the presence of the MIL-53(Fe) in the structure. On the basis of aforementioned analysis of XRD, XPS, FT-IR, SEM and TEM results, it can be identified that the successfully preparation of Fe_3S_4(52.1wt%)/MIL-53 hybrid catalyst with hierarchical nanostructure. As is known, the Fe_3S_4 has good electronic conductivity caused by its inverse spinel structure,[11a] thus facilitating the overall conductivity. Meanwhile, the substrate MIL-53(Fe) with loose skeleton not only can effectively prevent the agglomeration of the surface Fe_3S_4 nanosheets, but also enable intimate and large area contact with the electrolyte, which endow the Fe_3S_4(52.1wt%)/MIL-53 hybrid catalyst with the high exposure of active sites and fast electron transport in the HER process. In this regard, the formation of Fe_3S_4(52.1wt%)/MIL-53 hierarchical nanostructure with targeted two components provides an ideal platform to realize the effective regulation of HER activity.

To verify our speculation, electrochemical measurments of various Fe_3S_4(*x* wt%)/MIL-53 hybrid catalysts were performed in 0.5 M H_2SO_4 solution. Besides, we also synthesized Fe_3S_4 and tested its catalytic performance for comparison. As shown in Fig. 4a and Table S1, all of the Fe_3S_4(*x* wt%)/MIL-53 hybrid catalysts possess much lower onset overpotentials (η) than that of the pure MIL-53(Fe) and Fe_3S_4, among all Fe_3S_4(52.1wt%)/MIL-53 hybrid catalyst exhibits the lowest value of 48 mV, suggesting the superior HER activity. The overpotential that is required to achieve a current density of 10 mA cm^{-2} is a metric relevant to solar fuel conversion. Herein, the Fe_3S_4(52.1wt%)/MIL-53 hybrid catalyst exhibits a significantly low overpotential (η_{10}) of 92 mV, which is much

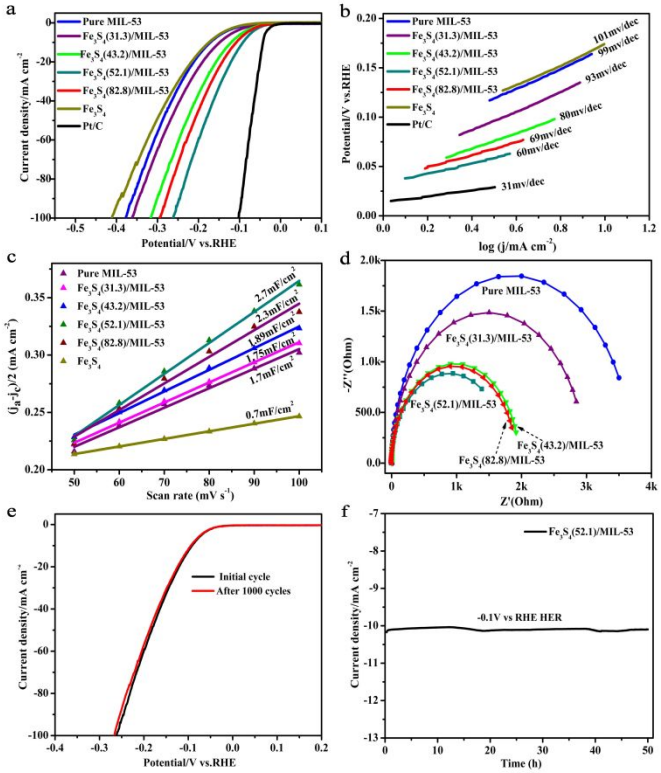

Fig. 4 (a) Polarization curves and (b) Corresponding Tafel plots of various samples as indicated. (c) The differences in current density variation (j_a-j_c) at an overpotential of 0.17 V plotted against scan rate, where the slope is twice C_{dl}. (d) Nyquist plots. (e) Polarization curves of the Fe_3S_4(52.1wt%)/MIL-53 hybrid catalyst initially and after 1000 CV cycles. (f) Time-dependence of current density of the Fe_3S_4(52.1wt%)/MIL-53 hybrid catalyst under a static overpotential of 100 mV.

smaller than that of the pure MIL-53(Fe) (172 mV) and Fe_3S_4 (185 mV) as well as other three synthesized hybrid catalysts (108-151 mV). As far as we know, these overpotentials mentioned above of Fe_3S_4(52.1wt%)/MIL-53 hybrid catalyst are also remarkable compared with recently reported values for metal sulfide-based electrocatalysts (Table S2), suggesting its excellent HER performance. The high catalytic activity is further illustrated by comparing the slopes of Tafel plots (Fig. 4b) for the Fe_3S_4(52.1wt%)/MIL-53 (60 mV $decade^{-1}$) with other counterparts (69-101 mV $decade^{-1}$), implying it could be more beneficial for practical application.

To further investigate the intrinsic HER activity of the Fe_3S_4(52.1wt%)/MIL-53 hybrid catalyst, the exchange current density (j_0) was obtained by applying the extrapolation method to the Tafel plots. As shown in Fig. S3 and Table S1, the j_0 for the Fe_3S_4(52.1wt%)/MIL-53 hybrid catalyst is determined as 363 μA cm^{-2}, which is larger than the values obtained for the other counterparts, suggesting the excellent activity for HER catalysis. This large j_0 could be attributed to the ideal hierarchical nanostructure and composition that can offer more effective active sites. Moreover, electrochemical double-

layer capacitances (C_{dl}), which are linearly proportional to the electrochemically active surface area,[13] were measured to evaluate the effective surface area of various samples by measuring their CV curves in the potential range from 0.1 to 0.2 V(Fig. 4c and Fig. S4). As shown in Fig. 4c and Table S1, Fe_3S_4 (52.1wt%)/MIL-53 hybrid catalyst exhibits much larger C_{dl} of 2.7 mF cm^{-2} than the other counterparts, showing the high exposure of effective active sites, which is responsible for the excellent HER activity.

To go further, the electrochemical impedance spectroscopy (EIS) was performed to reveal the electrode kinetics of the Fe_3S_4(*x* wt%)/MIL-53 hybrid catalyst under HER process. As shown in Fig. 4d, the Nyquist plots reveal a significantly decrease of semicircle diameter for the Fe_3S_4(52.1wt%)/MIL-53 in contrast to the pure MIL-53(Fe), Fe_3S_4(31.3wt%)/MIL-53 as well as the Fe_3S_4(43.2wt%)/MIL-53, indicating the low charge-transfer resistance at the catalyst/electrolyte interface and improved HER kinetics. This can be attributed to the enhancement of conductivity with high degree of sulfidation treatment. In addition, the charge-transfer resistance of Fe_3S_4(52.1wt%)/MIL-53 is also smaller than that of Fe_3S_4(82.8wt%)/MIL-53, which may arise from the ideal hierarchical nanostructural that enable intimate and large area contact with both the electrode and electrolyte. As a result, Fe_3S_4(52.1wt%)/MIL-53 hybrid catalyst possesses both rich effective active sites and good overall conductivity, which determine the superior HER activity.

Apart from the HER activity, stability is another significant criterion to estimate an advanced electrocatalyst. To evaluate the stability of the Fe_3S_4(52.1wt%)/MIL-53 hybrid catalyst in an acidic environment, long-term cycling test and continuous HER process at a static overpotential were performed. As shown in Fig. 4e, the polarization curves measured before and after 1000 CV cycles were compared. Negligible difference can be observed between the initial polarization curve and the final one, revealing the highly durability of the Fe_3S_4(52.1wt%)/MIL-53 hybrid catalyst. Moreover, when a constant overpotential of 100 mV is applied, a continuous HER process occurs to generate molecular hydrogen. As shown in Fig. 4f, the current density exhibits nearly unchanged even after a long period of 50 h. In addition, long-term soaking in 0.5 M H_2SO_4 for 50 h was also conducted to evaluate the chemical stability of the Fe_3S_4(52.1wt%)/MIL-53 hybrid catalyst in an acidic environment. As shown in Fig. S5, the XRD pattern of the acid soaked product indicates that no phase change occurs after acidic treatment. All of these results above prove that the Fe_3S_4(52.1wt%)/MIL-53 hybrid catalyst possesses excellent HER activity as well as superior stability, making it a promising HER catalyst for practical applications.

In summary, we have reported a controlled partial sulfurization strategy to prepare ultra-small Fe_3S_4 nanosheets attached on 3D MIL-53(Fe) hybrid catalysts for efficient HER via a facile solvothermal approach. By modulating the Fe_3S_4/MIL-53(Fe) ratio, the Fe_3S_4(52.1wt%)/MIL-53 hybrid catalyst with ideal hierarchical nanostructure and composition exhibited high HER activity with low overpotential of 92 mV at a current density of 10 mA cm^{-2}, small Tafel slope of 60 mV $decade^{-1}$ and high long-term durability in acid solutions. Our study will provide a valuable guideline for the design of MOF-based materials with optimized HER activity.

Acknowledgements

This work was supported by the NSF of China (No: 21673127, 21805165, 21671119, 51572152, and 51502155), NSRF of Hubei Provincial Education Office of China (No: Q20181203), the State Key Laboratory of Structural Chemistry, FJIRSM (20170020) and the 111 Project (2018-19-1).

Notes and references

1 M. S. Dresselhaus and I. L. Thomas, *Nature,* 2001, **414**, 332.
2 J. A. Turner, *Science,* 2004, **305**, 972.
3 (a) V. R. Stamenkovic, B. S. Mun, M. Arenz, K. J. J. Maryhofer, C. A. Lucas, G. Wang, P. N. Ross and N.M. Markovic, *Nat. Mater.,* 2007, **6**, 241; (b) L. He, J. Liu, Y. Liu, B. Cui, B. Hu, M. Wang, K. Tian, Y. Song, S. Wu, Z. Zhang, Z. Peng and M. Du, *Appl. Catal., B*, **2019**, *248*, 366-379.
4 (a) M. Jahan, Z. L. Liu and K. P. Loh, *Adv. Funct. Mater.,* 2013, **23**, 5363; (b) W. Wang, X. Xu, W. Zhou and Z. Shao, *Adv. Sci.,* 2017, **4**, 1600371; (c) J. S. Qin, D. Y. Du, W. Guan, X. J. Bo, Y. F. Li, L. P. Guo, Z. M. Su, Y. Y. Wang, Y. Q. Lan and H. C. Zhou, *J. Am. Chem. Soc.*,2015,**137**,7169;(d) Y. P. Wu, W. Zhou, J. Zhao, W. W. Dong, Y. Q. Lan, D. S. Li, C. Sun and X. Bu, Angew. Chem. Int. Ed., 2017, **56**, 13001. (e) B. Zhu, R. Zou and Q. Xu, *Adv. Energy. Mater.,* 2018, 27, 1801193; (f) T. Liu, P. Li, N. Yao, G. Cheng, W. Luo, S. Chen and Y. Yin, *Angew. Chem., Int. Ed.,* 2019, 10.1002/anie.201901409.
5 (a) S. L. Zhao, Y. Wang, J. C. Dong, C. T. He, H. J. Yin, P. F. An, K. Zhao, X. F. Zhang, C. Gao, L. J. Zhang, J. W. Lv, J. X. Wang, J. Q. Zhang, A. M. Khattak, N. A. Khan, Z. X. Wei, J. Zhang, S. Q. Liu, H. J. Zhao and Z. Y. Tang, *Nat. Energy*,2016, **1**,16184;(b) J. Q. Shen, P. Q. Liao, D. D. Zhou C. T.He, J. X. Wu, W.X. Zhang, J. P. Zhang and X. M. Chen, *J. Am. Chem. Soc.*, 2017, **139**, 1778.
6 (a) K. Jayaramulu, J.Masa, O. Tomanec, D. Peeters, V. Ranc, A. Schneemann, R. Zboril, W. Schuhmann and R. A. Fischer, Chan Kang, *Adv. Funct. Mater.*, 2017, **27**, 1700451; (b) Y. Guo, J. Tang, H. Qian, Z. Wang and Y. Yamauchi, *Chem. Mater.,* 2017, **29**, 5566.
7 X. Wang, H. Xiao, A. Li, Z. Li, S. Liu, Q. Zhang, Y. Gong, L. Zheng, Y. Zhu, C. Chen, D. Wang, Q. Peng, L. Gu, X. Han, J. Li and Y. Li, *J. Am. Chem. Soc.,* 2018, **140**, 15336.
8 (a) K. Cho, S-H. Han and M. P. Suh, *Angew. Chem. Int. Ed.,* 2016, **55**, 1; (b) Q. Lu, M. T. Zhao, J. Z. Chen, B. Chen, C. Tan, X. Zhang, Y. Huang, J. Yang, F. Cao, Y. Yu, J. Ping, Z. Zhang, X.-J. Wu and H. Zhang, *Small*, 2016, **12**, 4669.
9 F.-L. Li, Q. Shao, X. Huang and J.-P. Lang, *Angew. Chem., Int. Ed.,* 2018, **57**, 1888.
10 (a) L. Ai, L. Li, C. Zhang, J. Fu and J. Jiang, Chem. Eur. J., 2013, 19, 15105; (b) Y. Zhang, G. Li, H. Lu, Q. Lv and Z. Sun, RSC Adv., 2014, **4**, 7594.
11 (a) Y-J. Zhang, J. Qu, S-M. Hao, W. Chang, Q-Y. Ji and Z-Z. Yu, *ACS Appl. Mater. Interfaces*, 2017, **9**, 41878; (b) S-P. Guo, J-C. Li, J-R. Xiao and H-G. Xue, *ACS Appl. Mater. Interfaces*, 2017, **9**, 37694.
12 (a) C. H. Zhang, L. H. Ai and J. Jiang, *J. Mater. Chem. A*, 2015, **3**, 3074; (b) X. Zhao, X. Lan, D. Yu, H. Fu, Z. Liu and T. Mu, *Chem. Commun.,* 2018, **54**, 13010.
13 J. Xie, J. Zhang, S. Li, F. Grote, X. Zhang, H. Zhang, R. Wang, Y. Lei, B. Pan and Y. Xie, *J. Am. Chem. Soc.,* 2013, **135**, 17881.

Graphical Abstract-Pictogram

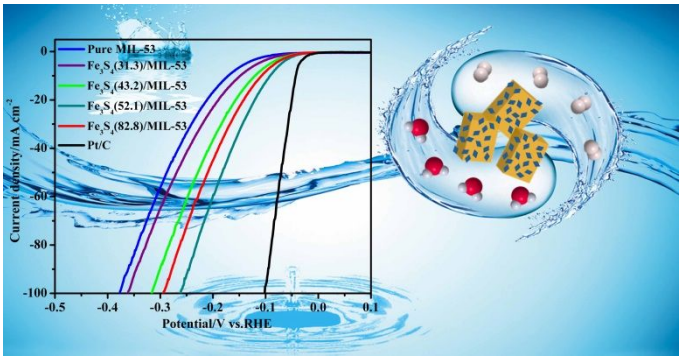

By modulating the Fe_3S_4/MIL-53(Fe) ratio with a controlled partial sulfurization strategy , the Fe_3S_4(52.1wt%)&MIL-53 hybrid catalyst with ideal hierarchical nanostructure and composition exhibited high HER activity with low overpotential of 92 mV at a current density of 10 mA cm^{-2}, small Tafel slope of 60 mV $decade^{-1}$ and high long-term durability in acid solutions. This work provides a new method for designing efficient and stable MOF-based electrocatalysts for HER